HHS Public Access

Author manuscript

Carbohydr Polym. Author manuscript; available in PMC 2021 April 01.

Published in final edited form as:

Carbohydr Polym. 2020 April 01; 233: 115828. doi:10.1016/j.carbpol.2020.115828.

Hypromellose Acetate Succinate based Amorphous Solid Dispersions via Hot Melt Extrusion: Effect of Drug Physicochemical Properties

Sandeep Sarabu[a], **Venkata Raman Kallakunta**[a], **Suresh Bandari**[a], **Amol Batra**[b], **Vivian Bi**[b], **Thomas Durig**[b], **Feng Zhang**[c], **Michael A. Repka**[a,d,*]

[a]Department of Pharmaceutics and Drug Delivery, The University of Mississippi, University 38677, USA

[b]Ashland Specialty Ingredients, Wilmington, DE 19808

[c]College of Pharmacy, The University of Texas at Austin, Austin, Texas 78712, USA

[d]Pii Center for Pharmaceutical Innovation and Instruction, The University of Mississippi, University 38677, USA

Abstract

In this study, the impact of drug and hydroxypropyl methylcellulose acetate succinate (HPMCAS) grades physicochemical properties on extrusion process, dissolution and stability of the hot melt extruded amorphous solid dispersions (ASDs) of nifedipine and efavirenz was investigated. Incorporation of drugs affected the extrusion temperature required for solid dispersion preparation. Differential scanning calorimetry and powder X-ray diffraction studies confirmed the amorphous conversion of the drugs in the prepared formulations. The amorphous nature of ASDs was unchanged after 3 months of stability testing at 40 °C and 75% relative humidity. The dissolution efficiency of the ASDs was dependent on the log P of the drug. The inhibitory effect of HPMCAS on drug precipitation was dependent on the hydrophobic interactions between drug and polymer, polymer grade, and dose of the drug. The dissolution rates were dependent on the solubility and hydrophilicity of the polymer grade.

Keywords

HPMCAS; Solid dispersions; HME; Nifedipine; Efavirenz; Supersaturation

1. Introduction

In the process of drug discovery combinatorial chemistry and high throughput approaches have been used to identify potential drug candidates (Williams et al., 2013). The majority of

*Corresponding author: Prof. Michael A. Repka, Tel: +1-662-915-1155, Fax: +1-662-915-1177, marepka@olemiss.edu.

these are either weak acids or weak bases and are identified as biopharmaceutical classification system (BCS) class-II drugs, exhibiting low solubility and high permeability(Lipinski, 2002; Tsume, Mudie, Langguth, Amidon, & Amidon, 2014; Williams et al., 2013). It is estimated that 40% of drugs in market and 90% of drugs in the discovery pipeline have poor water solubility(Kalepu & Nekkanti, 2015). Therefore, solubility and dissolution enhancement have become a common challenge for drug development. Several strategies have been developed to improve solubility: particle size reduction, salt formation for ionizable drugs, prodrugs, complexation, micellar systems and amorphous solid dispersions (ASDs) (Douroumis & Fahr, 2013; Fahr & Liu, 2007; Hancock, York, & Rowe, 1997). Among several strategies, drug amorphization is a promising approach to improve solubility and oral bioavailability(Tsume et al., 2014; Vasconcelos, Sarmento, & Costa, 2007). Several technologies such as hot melt extrusion (HME), spray drying, and Kinetisol® have been employed for the preparation of ASDs, However, only a few technologies are suitable for large/industrial scale operations, especially HME and spray drying (Mendonsa et al., 2019). HME has become an efficient process for the formulation and continuous manufacturing of ASDs (Kallakunta, Sarabu, Bandari, Tiwari, et al., 2019; Repka et al., 2018) and other novel drug delivery systems (Sarabu et al., 2019).

In the extrusion process, temperature and high shear force contribute to the dispersion of drug molecules in molten polymers forming a metastable dispersion or solid solution. Amorphous solids have high enthalpy, entropy and free energy, which enhances the solubility of the drugs(Friesen et al., 2008) compared to the crystalline counterpart. Since amorphous compounds are prone to crystallization upon storage, polymers must inhibit the crystallization process by: a)reducing the mobility of drug molecules, b)lowering the nucleation and crystallization process, c)increasing the activation energy of nucleation, and glass transition temperature (T_g) of the mixture. These mechanisms maximize the effect of supersaturation(Baghel, Cathcart, & O'Reilly, 2016; Konno, Handa, Alonzo, & Taylor, 2008).Solid dispersions with sui polymers act as supersaturating drug delivery systems and improve the intraluminal concentration of drugs beyond their saturation solubility and thereby the bioavailability of drug (Augustijns & Brewster, 2012).

Various polymers are used in the preparation of ASDs, including cellulosics, polyglycols (polyethylene glycol, polyethylene oxide), and polyvinyl polymers (polyvinyl alcohol, crospovidone, polyvinylpyrrolidone). Cellulose derivatives hydroxypropyl methylcellulose (HPMC) and hydroxypropyl methylcellulose acetate succinate (HPMCAS) contribute to two thirds of the solid dispersion-based market. Glass transition (T_g), thermal stability, and solubility are important factors that govern polymer performance. It is essential to select a suitable polymer which improves drug solubility and inhibits drug precipitation, such as HPMCAS(J. M. O. Pinto, Leão, Riekes, França, & Stulzer, 2018). HPMCAS is an enteric polymer commercially available in three grades; LG, MG, and HG. The key properties of HPMCAS are high T_g (119 °C-122 °C), amphiphilic nature, and insolubility in water and simulated gastric fluid, melt viscosity values are about 2.4-3.6 mPa.S. The grades of HPMCAS differ in their acetyl and succinoyl substitution (acetyl - 5-14%; succinoyl - 4-18%); LG, MG and HG dissolve at pH ≥ 5.5, 6.0 and 6.8, respectively("AquaSolve™ hydroxypropylmethylcellulose acetate succinate: Physical and chemical properties handbook," 2019; Sarode et al., 2014). There are many reports on the application of

HPMCAS as a carrier for solid dispersions prepared by spray drying, and KinetiSol® Dispersing. Solid dispersions were prepared by a solvent method for improving the bioavailability of poorly soluble nifedipine (NFD)(Tanno, Nishiyama, Kokubo, & Obara, 2004). In another study, solid dispersions of felodipine formulated with poly(vinylpyrrolidone), HPMC and HPMCAS were compared for the dissolution profiles(Konno et al., 2008). Out of the three polymers, HPMCAS provided the highest level of supersaturation for the greatest length of time. HPMCAS HF grade was successfully utilized in inhibiting the crystallization process of solid dispersions (SDs) prepared by melt solvent amorphization and HME process(Haware et al., 2019; Zhang et al., 2018).

The physicochemical properties of drugs and excipients (polymers) play a critical role in development of ASDs. Properties like particle size, Log P, melting temperature (T_m), pKa, T_g can affect the solubility and stability of formulation prepared via HME. Solubility and stability are the two key factors for the clinical performance of any drug(Dharani, Ali, Afrooz, Khan, & Rahman, 2019). T_m and T_g affect the processing temperature required for the preparation of ASDs, polymers with high T_g promote stability of ASDs. It is always challenging to prepare stable ASDs for drugs with low T_g (Kallakunta, Sarabu, Bandari, Batra, et al., 2019). In this context, it is essential to identify the potential effects of drug physicochemical properties on the solubility and stability of HPMCAS ASDs (Baghel et al., 2016; Gao & Shi, 2012; Vasconcelos et al., 2007). The novelty of this investigation was to formulate HME based ASDs for drugs (Nifedipine (NFD) & Efavirenz (EFZ)) with different physicochemical properties. Further, the effect of drug physicochemical properties and HME process variables on the solubility and stability of solid dispersions was investigated using a discriminatory dissolution method, and solid-state characterization tools, differential scanning calorimetry (DSC) and X-ray diffraction (XRD). The effect of dose and polymer grade on drug release characteristics was assessed and correlated with the physicochemical properties of the drugs.

2. Materials and methods

2.1. Materials

HPMCAS (Aquasolve™) was supplied by Ashland, Inc. (Lexington, KY, USA). HPMCAS, a synthetic polymer, is a mixture of acetic acid and monosuccinic acid esters of hydroxypropylmethyl cellulose. It is commercially available in three chemical grades and two physical grades. The three chemical grades L, M and H vary in their acetyl and succinoyl group substitution. The two physical grades include fine and granular which differ in their particle size and are coded as F and G respectively. HPMCAS has four substituent groups: methoxyl, hydroxypropoxy, acetyl, and succinoyl. The range of substitution on each grade and their key physicochemical properties are listed in Table 1a. For this study, the commercially available grades HPMCAS LG, HPMCAS MG and HPMCAS HG were utilized. NFD and EFZ were donated by Ashland, Inc. All other chemicals used were analytical reagent grade.

2.2. Methods

2.2.1. Solubility Studies—The solubility studies for NFD and EFZ were performed in pH 6.8 phosphate buffer and water. For EFZ, additional studies were performed in 1% sodium lauryl sulfate (SLS) in water, 1% SLS in the pH 6.8 phosphate buffer and 0.25% SLS in the pH 6.8 phosphate buffer. An excess of drug was added to 10 mL of each aqueous solution, and the solutions were shaken (Taitec Bioshaker., Saitamaken, Japan) for 48 hours at 100 RPM and 37 °C. Then, the samples were centrifuged at 13000 RPM for 15 minutes and the supernatant was filtered through a 0.45 μm PVDF membrane filter (Durapore®; Millpore Sigma, MA, USA) and diluted with respective media for quantification of drugs by UV-Vis spectrophotometry (Genesys 6, Thermo Scientific, USA) with absorbance measured separately at 340 nm and 247 nm for NFD and EFZ respectively. All tests were performed in triplicates.

2.2.2. Thermal characterization—DSC analysis was performed to determine the T_m and T_g of NFD, EFZ and HPMCAS. DSC studies were carried out using Discovery DSC 25 (TA Instruments DSC, New Castle, DE, USA), coupled with a RCS90 cooling device. The instrument was calibrated for temperature and heat capacity using indium and sapphire standard. All samples weighed approximately 5-10 mg and were sealed in an aluminum pan. The samples were equilibrated under nitrogen gas for one minute at 25 °C and then heated at a rate of 10 °C/min under an inert nitrogen purge of 50 mL/min. The thermograms were analyzed to detect the melting temperature and T_g.

2.2.3. HME processing

2.2.3.1. Pure polymer extrusion: The raw materials that passed through a USP #25 mesh sieve were used for extrusion. HPMCAS polymer grades (LG, Mg and HG) were extruded in the temperature range of 150 °C-180 °C using an 11-mm co-rotating twin-screw extruder (Thermo Fisher Scientific, Waltham, MA, USA). A Thermo Fisher standard screw configuration consisting of 3 mixing zones at a screw speed of 50 RPM and feed rate of 2.5 g/min was employed for extrusion. The process parameters were recorded.

2.2.3.2. HPMCAS ASDs: Drug-polymer (30% w/w drug) binary mixtures were prepared for both drugs with LG, MG and HG separately. These mixtures were blended using a V-shell blender (Maxiblend, GlobePharma), then extruded in the temperature range 130 °C to180 °C, 130 °C to 150 °C for NFD and EFZ respectively using extruder screw configuration and feed rate as mentioned in the pure polymer extrusion. A screw speed of 50 RPM and 100 RPM was used in preparation of NFD and EFZ ASDs respectively. The obtained extrudates were milled using a laboratory grinder, sieved using a #30 ASTM mesh for NFD, #30 and #40 ASTM mesh for EFZ, and stored in amber colored bottles at room temperature.

2.2.4. Solid state characterizations—Solid state characterization was performed to confirm the formation of amorphous ASDs of NFD and EFZ.

2.2.4.1. DSC: DSC studies were performed to investigate the drug-polymer miscibility and thermal behavior of the prepared formulations. Drug-polymer miscibility is key factor for

the formation of stable ASDs. Pure drugs, physical mixtures, and formulations were subjected to DSC studies. All the prepared formulations were investigated via a heat-cool-heat cycle. In the first heating cycle, the samples were heated to 200 °C at a heating ramp of 10 °C/min, and then the samples were cooled to 10 °C and −40 °C for NFD and EFZ samples, respectively. Finally, the samples were heated to 135 °C at a slow heating ramp of 1 °C/min to detect the T_g.

2.2.4.2. Powder X-ray diffraction measurement (PXRD): PXRD studies were performed for pure drugs and milled extrudates using Rigaku X-ray system (D/MAX-2500PC, Rigaku Corporation, Tokyo, Japan) equipped with a copper tube anode and a standard sample holder. Diffraction measurements were performed under: CuKα radiation, 40-kV voltage, and 40 mA current. The 2θ scanning range was 2–50°, step width of 0.02°/S at a scanning speed of 2°/min. Samples placed on a sample holder were gently compressed with a clean metal bar and diffractograms were collected at room temperature (20-25 °C).

2.2.4.3. Fourier transform infrared spectroscopy (FTIR): FTIR studies were performed on an Agilent Cary 660 FTIR Spectrometer (Agilent Technologies, Santa Clara, CA, USA). To study the interaction between the drug and polymer, a small amount of sample placed on top of diamond crystal was pressed with a MIRacle high-pressure clamp, and the spectrum was collected in the range of 600–4000 cm^{-1} with 16 scans and a resolution of 4 cm^{-1}. The FTIR bench was equipped with an ATR (Pike Technologies, Madison, WI, USA), which was fitted with a single-bounce, diamond-coated ZnSe internal reflection element.

2.2.5. In-vitro drug release studies

2.2.5.1. Dissolution of formulations: In-vitro drug release studies for NFD were performed at 20 mg, 67.5 mg and 135 mg in 900 mL of a pH 6.8 phosphate buffer using USP apparatus type II (SR8-plus™, Hanson), maintained at 37 ± 0.5 °C with a paddle speed of 50 RPM for 2 h (n = 3). For EFZ, a dose equivalent to 100 mg of EFZ was used for the in vitro release studies performed in a pH 6.8 phosphate buffer, pH 6.8 phosphate buffer + 1% SLS, and pH 6.8 phosphate buffer +0.25% SLS using USP apparatus type II (SR8-plus™, Hanson) maintained at 37 ± 0.5 °C. The volume of media used was 1000 mL, with a paddle speed of 50 RPM for 2 h. Sample aliquots (3 mL) were collected at 15, 30, 45, 60, 90 and 120 minutes and replaced with an equivalent volume of fresh media maintained at 37 ± 0.5 °C for both drugs. The samples were filtered through a 0.45μm PVDF membrane (Durapore®; Millpore Sigma, MA, USA) filter and estimated for drug concentration by UV spectrophotometry with absorbance measured separately at 340 nm and 247 nm for NFD and EFZ respectively against the dissolution medium as blank.

2.2.5.2. Treatment of dissolution data: From the dissolution profiles, various dissolution parameters such as dissolution efficiency (DE), initial dissolution rate (IDR) and mean dissolution rate (MDR) were calculated (Eedara, Veerareddy, Jukanti, & Bandari, 2014). The dissolution efficiency (DE) is calculated as the percentage ratio of the area under the dissolution curve up to a time (t), to that of the area of the rectangle described by 100% dissolution at the same time point. DE at 15, 30 and 60 minutes were calculated by using the following equation (1)

$$DE = \frac{(\int_0^t y \times dt)}{y_{100} \times t} \times 100\,\% \quad (1)$$

IDR was calculated for the first 15 min of dissolution using the following equation (2)

$$IDR = \frac{\%\ dissolved}{min} \quad (2)$$

MDR was calculated using the following equations (3)

$$MDR = \frac{\sum_{j=1}^{n} \Delta Mj\ /\ \Delta t}{n} \quad (3)$$

Where j is the dissolution sample number, n is the number of dissolution sampling times, Δt is the time at midpoint between two consecutive time points (t_j and t_{j-1}) and ΔM_j is the additional amount of drug released between two consecutive time points (t_j and t_{j-1}).

2.2.6 Stability studies—The HPMCAS-NFD, HPMCAS-EFZ ASD formulations prepared at temperatures 170°C and 150°C respectively were subjected to stability studies at accelerated stability conditions (40 °C and 75% relative humidity (RH)) for 3 months. Samples collected from the stability chamber (Caron, 6030) at 1 and 3 months were observed for physical appearance and tested for amorphous nature, drug content and dissolution. The similarity factor (f_2) was calculated using following equation (4):

$$\mathbf{f_2 = 50 \log \{[1 + (1\ /\ n) \Sigma_{t\,=\,1\text{-}n} (R_t\text{-}T_t)^2]^{0.5} \times 100\}} \quad (4)$$

where,

R_t = cumulative drug release of initial samples,

T_t = cumulative release of test sample at predetermined time points,

N = number of time points

The f_2 value ranges from 1 to 100: higher the f_2 value, higher the similarity. A f_2 value of greater than 50 is considered similar(Kallakunta, Patil, Tiwari, Ye, et al., 2019).

3. Results and discussion

3.1. Solubility studies

In this study, NFD showed a solubility of 14.97±3.98 mg/L and 14.01 ± 3.52 respectively in pH 6.8 PB and water respectively. EFZ exhibited higher solubility values in the media with surfactant, 2.33±0.32, 2.32±0.08 mg/mL and 0.63±0.01 mg/mL in water+1%SLS, pH 6.8 PB+1%SLS, pH 6.8 PB+0.25%SLS, respectively. Whereas it was only 1.96 ± 0.15 and 6.67 ± 0.69 mg/L without SLS. NFD had a higher aqueous solubility than EFZ, this agreed with

the literature, where EFZ had a higher log P of 4.5-5.4, whereas NFD had a log P of 2.5(Curley et al., 2017; Tanaka et al., 2008; Van Der Lee et al., 2001). The solubility values determined for EFZ agree with the values reported in the literature (Cristofoletti et al., 2013; E. C. Pinto, Cabral, & de Sousa, 2014), the solubility increased with the increase in surfactant concentration.

3.2. Thermal characterization

Thermal analytical techniques provide data about thermal stability, melting and recrystallization temperatures(Marasini et al., 2013). The sharp endothermic peaks at 175.04 °C and 138.86 °C correspond to the melting points of NFD and EFZ respectively (Figure 1 and Figure 2). The heat-cool-heat cycle showed another endothermic peak for NFD at 42.18 °C and EFZ at 30.5 °C (supplementary data: Figure S1a and S1b), which corresponds to the T_g of NFD and EFZ respectively. The results of thermal analysis agreed with the reported melting temperatures of 172-174 °C for commercially available NFD polymorph I (Filho, Franco, Conceição, & Leles, 2009; Leite et al., 2013; Macêdo, Gomes do Nascimento, Soares Aragão, & Barreto Gomes, 2000) and 138.51 °C for EFZ(Fandaruff et al., 2014).

For HPMCAS grades, no thermal events were detected in the 25-220 °C heating cycle, confirming the amorphous nature. A transition observed during the reheat cycle corresponds to the T_g of the three grades, determined to be between 119.0 – 122.52 °C. The above results are in accordance with the literature and confirm the purity of materials studied(Sarode et al., 2014).

3.3. HME Processing

3.3.1. Pure polymer extrusion—The grades of pure HPMCAS were extruded to investigate the feasibility of HPMCAS extrusion. The extrusion was feasible at temperatures ≥ 170 °C. At temperatures < 170 °C, the torque values were greater than 85%. The ease of extrusion was based on the experimental torque values obtained at different processing temperatures. The ease of extrusion was in the order: HG > MG > LG. For extrusion at the temperature range of 180-190 °C, a change in texture of the polymer extrudates was observed. This may be due to change in the physicochemical properties of the polymer or due to an increase in the total free acid content during the extrusion process, due to the release of free succinic acid, HPMCAS LF grade was reported to yield the lowest increase in total acid content after extrusion(Sarode et al., 2014). Pure polymer extrusion observations (Table 1b) were utilized in optimizing the processing temperatures for NFD and EFZ ASDs.

3.3.2. HPMCAS-drug formulations—For NFD formulations, it was observed that 150 °C was the lowest temperature at which they could be extruded, considering the high process torque values (> 85%) that were obtained at temperatures below 150 °C. In extrusion, NFD has shown plasticization, which facilitated extrusion at 150 °C. At temperatures ≥ 180 °C, a change in the surface texture of the NFD extrudates was like pure polymer extrudates. The HG formulations were extruded with less process torque than the LG and MG, indicating the ease of HG extrusion. Formulations extruded at process temperatures of 150-170 °C were further evaluated and subjected to accelerated stability studies.

EFZ has poor flow properties, but the physical blend with 70% (w/w) HPMCAS and 30% (w/w) EFZ exhibited improved flow properties. The angle of repose values for EFZ and the 30% (w/w) physical blend were 54° (poor) and 39° (Fair), respectively. EFZ has shown a better plasticization compared to NFD, which might be due to a lower melting temperature than NFD. Formulations were successfully extruded with process temperatures ranging between 130-150 °C at a screw speed of 100 RPM, whereas at 50 RPM the process was slow. The formulations prepared at 100 RPM were further evaluated and subjected to stability studies. The temperatures used and the torque values are given in Table 1b.

3.4. Solid state characterizations

3.4.1. DSC and PXRD—ASDs are thermodynamically metastable systems. During storage there is high chance for the spontaneous recrystallization of the drug resulting in loss of its performance. It is assumed that completely miscible single-phase amorphous systems offer enhanced solubility and stability (Semjonov et al., 2017). The miscibility of a drug is determined by the T_g. The T_g of the binary mixture can be predicted using the Fox equation (5) based on the T_g and weight fractions (ω) of pure components as given below

$$\frac{1}{T_g} = \frac{\omega 1}{T_g 1} + \frac{\omega 2}{T_g 2} \quad (5)$$

Where T_g is the glass transition temperature, ω_1 and ω_2 are the weight fractions of the components.

A single T_g of 73-74 °C and 69-70 °C was observed in the NFD and EFZ formulations, respectively (Figure 1d and Figure 2d). This confirms the miscibility of the drug and polymer, and the presence of a single phase indicates the molecular dispersion of the drug in the polymer matrix. The experimental T_g values were close to the ones predicted using fox equation.

In the physical mixtures (PM), melting endotherms with reduced intensities were observed. The melting endotherms disappeared in the NFD and EFZ formulations, indicating the amorphous conversion of active pharmaceutical ingredients (APIs) (Figure 1 and Figure 2). This was further confirmed by PXRD studies.

In PXRD studies, NFD had major characteristic peaks at 8.15°,11.87°, 16° to 20° and at 35.91° (Figure 3a). EFZ showed a sharp peak at 6.17° and small peaks at 11.01°,10.49° and 20.17° (Figure 3b). The characteristic peaks of NFD and EFZ were not detected in the diffractograms of formulations (Figure 3a & 3b). These results correlate with the DSC results, confirming the amorphous nature of the drugs in prepared ASDs. Amorphous conversion of APIs in prepared formulations is attributed to the dispersion of molten drug at the molecular level in the polymer matrix.

3.4.2. FTIR—HME process does not affect the functional groups in the solid state of polymer. Thus, polymer can still involve in non-covalent interactions with the drugs(Sarode et al., 2014). FTIR spectra were used to characterize the drug-polymer hydrogen bonding in the HPMCAS-NFD and HPMCAS-EFZ solid dispersions. The characteristic peak at 3324

cm^{-1} in NFD corresponded (Figure 4a) to the dihydropyridine N-H stretch, which acted as the hydrogen bond donor(Tang, Pikal, & Taylor, 2002) and was involved in hydrogen bonding with polymers. The peaks at 1677 cm^{-1} and 1647 cm^{-1} corresponded to the C=O and C=C stretch, respectively. The peak due to the N-O symmetric stretch 1530 cm^{-1} was observed in NFD and the HPMCAS-NFD solid dispersions. In the NFD solid dispersions, new broad peaks were observed at 1727 cm^{-1} and 1692 cm^{-1}, which indicated an interaction between the drug and polymer as reported for HPMCAS and NFD(Kothari, Ragoonanan, & Suryanarayanan, 2014), due to hetero-molecular interactions on the C=O group or loss of intramolecular hydrogen bonding(Cilurzo, Minghetti, Casiraghi, & Montanari, 2002; Tanno et al., 2004; Tominaga, 2013). The reduced intensity of the N-H stretch peak in solid dispersions might be attributed to the molecular distribution of NFD in the HPMCAS polymers.

In the IR spectrum of EFZ, the characteristic peaks at 2248 cm^{-1}, 1000-1400 cm^{-1}, and 3313 cm^{-1} represent the alkyne peak, C-F, and the N-H stretch, respectively (Figure 4b). HPMCAS has multiple hydrogen bond acceptor sites(Kothari et al., 2014) that can form hydrogen bonds with EFZ in the prepared formulations. A sharp peak at 1742 cm^{-1}, characteristic to EFZ, shifted lower to 1737 cm^{-1} in prepared formulations. The peak broadening and reduced intensity indicated hydrogen bonding between the drug and the polymer.

3.5. *In vitro* dissolution study of NFD formulations

3.5.1. Effect of dose on dissolution profile—The dissolution studies were conducted with 20 mg equivalent dose of NFD in 900 mL of the pH 6.8 phosphate buffer. For this study, pure NFD and formulations extruded at 170 °C were used. At this dose, LG and MG formulations showed similar dissolution profiles (f_2>50; 77.7) at 90 min, with 96.6 ± 4.16 % and 99.6 ± 3.25 % drug release, respectively (Figure 5a). In the HG formulations, the dissolution profile was 51% at the end of 2 h, whereas the pure drug showed approximately 1% drug release at the end of 2 h. The slow release with the HG might be attributed to the solubility and slow ionization rate of HG in the pH 6.8 phosphate buffer compared to the LG and MG(Sarode et al., 2014).

The saturation solubility of NFD in the pH 6.8 phosphate buffer was found to be 14.97 ± 3.98 mg/L. Precipitation is a rate limiting step of the dissolution process of a solid dispersion system. To evaluate the precipitation inhibition efficiency of polymer, along with the 20 mg dose dissolution was also performed at a dose equivalent to 5 times (67.5 mg) and 10 times (135 mg) the saturation solubility. At a dose equivalent to 135 mg of NFD, the % drug release reached a maximum of 74.76 ± 2.65 in 30 min and 74.72 ± 1.57 at 60 min for formulations prepared with LG and MG, respectively. After 30 min, with the LG formulations precipitation was visually observed in the dissolution vessel and the concentrations of dissolved drug in the vessel dropped to 33.34 ± 3.00 and 68.09 ± 3.84 at the end of 2 h in LG and MG, respectively (Figure 5C). The rate of supersaturation and rate of precipitation was rapid in the LG formulations compared to the MG formulations. Drug release was slow (23-25% after 2 h) in HG NFD and there was no sign of precipitation as the release did not reach the maximum value.

No signs of drug precipitation were observed at a 67.5 mg equivalent dose of NFD at 2 h for both LG and MG formulations. The % drug release was 84.72 ± 1.46, 96.57 ± 1.61, 29.04 ± 0.49 for MG-NFD, LG-NFD and HG-NFD, respectively (Figure 5b). A higher initial release was observed in the LG formulations, and a maximum release was observed in the MG formulations. The difference in dissolution rates is because LG is more ionized in pH 6.8 phosphate buffer because of its higher succinoyl content and lower acetyl contents compared to the MG and HG grades(Ueda, Higashi, Yamamoto, & Moribe, 2013, 2014). From the dissolution profiles, various dissolution parameters such as dissolution efficiency (DE) and mean dissolution rate (MDR) were calculated (Eedara et al., 2014). The summary of dissolution parameters is in Table 2.

The dissolution efficiency (DE), mean dissolution rate (MDR) and initial dissolution rate values (IDR) of the formulations LG, MG and HG were significantly ($p<0.05$) improved, compared to the pure NFD. LG had the highest DE, MDR and IDR values followed by MG and HG at all the tested doses

3.5.2. Effect of processing temperature on dissolution profile of NFD formulations—In order to see the effect of processing temperature on drug dissolution and supersaturation maintenance, formulations were prepared at 160 °C and 170 °C. Dissolution studies were performed at a dose equivalent to 135 mg of NFD. The LG and MG formulations processed at 170 °C have higher drug release ($f2 < 50$; 48.01 and 47.42 for LG and MG respectively) with better supersaturation maintenance than the formulations processed at 160 °C (Figure 6). This might be because 170 °C is closer to the melting point of NFD, relatively greater fluidization of the polymer chains compared to at 160 °C, better dispersion of drug in polymer matrix(Ma et al., 2019). However, no effect of processing temperature was observed for the HG formulations. At 160 °C and 170 °C HG formulations have similar release profiles ($f2 > 50$; 90.01), which could be attributed to low solubility of HG in pH 6.8 phosphate buffer and an increase in disintegration time for the polymer with the increase in processing temperature (Sarode et al., 2014).

It was observed that LG-NFD formulations had high initial dissolution rates compared to MG. NFD precipitation was predominant in the LG formulations, and slight precipitation was observed in the MG formulations. All three grades of HPMCAS improved the solubility of NFD, with significant improvement in dissolution efficiency and initial dissolution rates with LG and MG. MG was found to be an effective polymer, with better dissolution and supersaturation maintenance(Tanno et al., 2004).

3.5.3. EFZ formulations—HPMCAS-EFZ formulations prepared at 150° C and 100 RPM were used for dissolution studies at a dose equivalent to 100 mg of EFZ, as it is one of the prescribed doses. The USP recommended dissolution media for tablet and capsule formulations are 1% SLS in water and 2% SLS in water respectively. For HPMCAS-EFZ formulations, both non-sink and sink dissolutions were performed in a pH 6.8 phosphate buffer and a pH 6.8 phosphate buffer + SLS, respectively. The sink and non-sink dissolution medium for EFZ were determined based on the solubility values. The solubility of EFZ was 6.7 mg/L, 620 mg/Land 2322 mg/L in pH 6.8PB, pH 6.8PB+0.25% SLS and pH 6.8PB+1% SLS respectively. As the dissolution dose is equivalent to 100 mg EFZ, pH 6.8 PB is a non-

sink dissolution medium and the media with surfactant concentration of 0.25% and 1% SLS are sink dissolution conditions.

3.5.3.1 Non-sink dissolution in pH 6.8 phosphate buffer: Non-sink dissolution studies were conducted in a pH 6.8 phosphate buffer. The % drug release was 62.96 ± 3.17, 17.58 ± 0.57, 2.9 ± 0.14 and 8.49 ± 0.32 after 2 h for LG-EFZ, MG-EFZ, HG-EFZ and pure EFZ, respectively (Figure 7a). The dissolution increased approximately 7-fold with LG and 2-fold with MG. Whereas less drug release was observed with the HG formulations. MG EFZ and HG EFZ had similar dissolution profiles with the pure EFZ (f2>50; 57.87 between MG-EFZ and EFZ API and 66.61 between HG-EFZ and EFZ API). This dissolution behavior could be due to a) lower solubility of the HG than LG and MG in pH 6.8 phosphate buffer; b) poor aqueous solubility of EFZ; and c) non-sink dissolution conditions.

3.5.3.2 Selection of discriminatory dissolution media for EFZ formulations: In the pH 6.8 phosphate buffer + 1% SLS dissolution media, a discrimination was not established. Even though the drug release improved for the LG-EFZ formulations, MG-EFZ and HG-EFZ still had similar dissolution profiles (f_2 >50; 52.64) (Figure 7b). The slow dissolution with the HG and MG even at 1% SLS could be due to lower solubilization with these grades and due to the relatively lower particle size of the EFZ compared to extrudates.

It was understood that: 1) EFZ API exhibited sink dependent dissolution; and 2) LG polymer could improve the dissolution of EFZ. The next study was aimed at identifying dissolution media with reduced surfactant concentration (pH 6.8 phosphate buffer + 0.25% SLS) to see the solubilizing capacity of the polymer grades and establish discrimination in release profiles. For this study the extrudates with reduced particle size (#40 ASTM mesh) were used.

3.5.3.3 Dissolution in pH 6.8 phosphate buffer + 0.25% SLS: A higher initial dissolution rate was observed with the LG-EFZ formulations than the other formulations and pure EFZ. The % drug release values were 80.39 ± 4.83, 68.42 ± 3.82, 17.14 ± 0.85, 34.35 ± 3.30 after 60 min and 91.81 ± 2.97, 94.03 ± 2.62, 30.03 ± 1.21 and 40.74 ± 2.56 after 2 h for LG-EFZ, MG-EFZ, HG-EFZ and pure EFZ, respectively (Figure 7c). In this dissolution medium, a clear discrimination (f_2< 50) was found between the LG-EFZ, MG-EFZ, HG-EFZ formulations and pure EFZ. The f_2 values for LG-EFZ formulations when compared to the release profiles of MG-EFZ, HG-EFZ formulations and API were 48.11, 13.12 and 20.43 respectively. Similarly, the f2 values were 16.38, 23.46 and 37.46 for the MG-EFZ to HG-EFZ, MG-EFZ to pure EFZ and HG-EFZ to pure EFZ respectively. These values confirmed the suitability of pH 6.8 phosphate buffer+0.25% SLS as the discriminatory dissolution media for evaluation of HPMCAS-EFZ formulations.

It can be concluded that EFZ API exhibited a sink dependent dissolution, LG and MG had a positive impact on the dissolution performance. Whereas with the HG, the dissolution was less than that of pure EFZ in all the three dissolution medium, this is attributed to the lower solubility/ionization of HG at pH 6.8, molecular level hydrophobic interactions between the HPMCAS HG and the aromatic moieties of the drug EFZ in the solid state during the extrusion process resulting in slower dissolution (Ueda et al., 2013). For dissolution, a pH

6.8 phosphate buffer + 0.25% SLS was chosen as a dissolution media for further evaluation of fresh and stability samples.

From the dissolution results, in non-sink conditions (pH 6.8 phosphate buffer), only LG solubilized EFZ while the MG and HG grades demonstrated similar dissolution profiles to EFZ API ($f_2 > 50$). On the other hand, NFD is solubilized by all the three polymer grades. The drug concentrations achieved in dissolution are influenced by several factors, including hydrophobic interactions between drug and polymer, extrusion processing conditions, acetyl to succinoyl ratio of the polymer, and ionization of the polymer at pH 6.8. In this study, EFZ being more hydrophobic forms a stronger hydrophobic interaction with the acetyl groups on the polymer resulting in slower dissolution. Even though the LG solubilized both of the drugs, a rapid supersaturation followed by a rapid decrease in drug concentration owing to a supersaturation-induced precipitation was observed with NFD whereas for EFZ the drug release was gradual or showing a slow rate of supersaturation resulting in a broader maximum kinetic solubility drug dissolution. The $AUC_{0\text{-}2}$ values for the LG NFD and LG EFZ formulations were 0.143 and 0.091 μg h/mL respectively(Sun & Lee, 2013, 2015). EFZ is less solubilized with the MG and HG grades but was able to maintain the concentrations achieved due to sink condition(Ueda et al., 2014). The dissolution with HG-EFZ formulations was less than EFZ API. This observation was in accordance with the literature. HPMCAS-HF was reported as a stabilizer due to its high Tg and least hygroscopic nature rather than a solubilizer in hot melt extruded EFZ solid dispersions (Pawar, Tayade, Gangurde, Moravkar, & Amin, 2016). In this reported study, complete drug release was achieved in less than 1 hour with Soluplus® favoring dissolution and HF acted as a stabilizer.

For NFD, polymer hydrophobicity, dissolution dose and drug polymer interaction appeared to be key factors in the supersaturation maintenance. No signs of precipitation were seen at 5 times the saturation solubility dose for 2h. MG generated extended supersaturation compared to LG in the fresh and stability samples of NFD. Succinoyl groups (hydrophilic region) of the polymer promote aqueous solvation whereas the acetyl and methoxyl groups (hydrophobic regions) interact with the drug and are responsible for precipitation inhibition of the drug from a supersaturated solution(Ilevbare, Liu, Edgar, & Taylor, 2012b, 2012a). A balance between these two characteristics aids in reaching supersaturation and maintaining it. The results of this study agree with the hydrophilicity/ hydrophobicity order of the polymer grades and the literature reports(J. M. O. Pinto et al., 2018). In this study, the pKa values for NFD (weak base) and EFZ (weak acid) were 3.93(Friedrich, Nada, & Bodmeier, 2005) and 10.2(Cristofoletti et al., 2013) respectively. (HPMCAS is an anionic polymer). These drugs may have interacted differently in the solid state with the anionic polymer, affecting the dissolution and supersaturation achieved with the respective drug. The results of this study agree with the difference in dissolution and supersaturation results achieved for solid dispersions of Indomethacin (weak acid) and Itraconazole (weak base) prepared with HPMCAS LF and HPMCAS HF (Sarode, Sandhu, Shah, Malick, & Zia, 2013).

In the prepared formulations, MG grade for NFD and LG grade for EFZ were found to be the best formulations because of their ability to attain maximum solubility and the ability to maintain supersaturation for prolonged duration.

3.6. Stability studies

The prepared formulations were stable at 40 °C and 75% RH for 3 months. No thermal events were observed in the DSC thermograms of NFD and EFZ (Figure 8), confirming the existence of the drugs in amorphous form. The drug content (%) values in all the formulations was found to be between 98.98±1.24 to 102.68±0.92, indicating the stability of formulations under accelerated conditions. The in-vitro drug release studies performed after 3 months showed similar release profiles (supplementary data: Figure S2) to the initial samples. The similarity factor values were greater than 50, substantiating the similarity of release profiles and stability of the samples. For the LG-EFZ formulation, the f2 values were found to be 51.21 which was on the low side. This observation might be due to more hygroscopicity of LG grade than MG and HG grades. This resulted in formation of granular compacts in the 3 months stability samples. These results suggest the use of desiccants during storage may be needed.

4. Conclusion

HPMCAS has emerged as a polymer to prepare stable ASDs and as a precipitation inhibitor. However, its use has been limited to ASDs prepared by spray drying considering the high processing temperatures required for use in HME. In this study, HPMCAS was successfully used as an amorphous carrier in the HME process to achieve improved solubility and supersaturation levels for NFD and EFZ. With the same polymer grade and under similar dissolution conditions, the extent of solubilization of different drugs is more dependent on the aqueous solubility/log P value of the drug. In this study, EFZ has a higher log P, it is accommodated well in the hydrophobic regions of the polymer and is less solubilized compared to NFD. The dissolution efficiency and initial dissolution rates were high for NFD ASDs compared to EFZ ASDs. The formulations prepared with NFD and EFZ formed stable ASDs. To conclude, identifying the right polymer grade based on the physicochemical properties of the API that can provide a greater shelf-life and maintain the supersaturated state for an extended period is important to improve the bioavailability of poorly soluble drugs. The impact of the study provides insight for the selection of a suitable HPMCAS grade and feasible HME processing conditions required for the development of stable ASDs for drugs with different physicochemical properties.

Supplementary Material

Refer to Web version on PubMed Central for supplementary material.

Acknowledgements

This project was also partially supported by Grant Number P30GM122733-01A1, funded by the National Institute of General Medical Sciences (NIGMS) a component of the National Institutes of Health (NIH) as one of its Centers of Biomedical Research Excellence (COBRE).

References

AquaSolve™ hydroxypropylmethylcellulose acetate succinate: Physical and chemical properties handbook. (2019, 8 21). Retrieved August 21, 2019, from https://www.ashland.com/file_source/

Ashland/Industries/Pharmaceutical/Links/PC-12624.6_AquaSolve_HPMCAS_Physical_Chemical_Properties.pdf

Augustijns P, & Brewster ME (2012). Supersaturating drug delivery systems: fast is not necessarily good enough. Journal of Pharmaceutical Sciences, 101(1), 7–9. [PubMed: 21953470]

Baghel S, Cathcart H, & O'Reilly NJ (2016). Polymeric amorphous solid dispersions: a review of amorphization, crystallization, stabilization, solid-state characterization, and aqueous solubilization of biopharmaceutical classification system class II drugs. Journal of Pharmaceutical Sciences, 105(9), 2527–2544. [PubMed: 26886314]

Cilurzo F, Minghetti P, Casiraghi A, & Montanari L (2002). Characterization of nifedipine solid dispersions. International Journal of Pharmaceutics, 242(1–2), 313–317. [PubMed: 12176270]

Cristofoletti R, Nair A, Abrahamsson B, Groot DW, Kopp S, Langguth P, … Dressman JB (2013). Biowaiver monographs for immediate release solid oral dosage forms: efavirenz. Journal of Pharmaceutical Sciences, 102(2), 318–329. [PubMed: 23175470]

Curley P, Rajoli RK, Moss DM, Liptrott NJ, Letendre S, Owen A, & Siccardi M (2017). Efavirenz is predicted to accumulate in brain tissue: an in silico, in vitro, and in vivo investigation. Antimicrobial Agents and Chemotherapy, 61(1), e01841–16. [PubMed: 27799216]

Dharani S, Ali SFB, Afrooz H, Khan MA, & Rahman Z (2019). Development and validation of a discriminatory dissolution method for rifaximin products. Journal of Pharmaceutical Sciences, 108(6), 2112–2118. [PubMed: 30685397]

Douroumis D, & Fahr A (2013). Drug delivery strategies for poorly water-soluble drugs. Wiley Online Library.

Eedara BB, Veerareddy PR, Jukanti R, & Bandari S (2014). Improved oral bioavailability of fexofenadine hydrochloride using lipid surfactants: ex vivo, in situ and in vivo studies. Drug Development and Industrial Pharmacy, 40(8), 1030–1043. [PubMed: 23738504]

Fahr A, & Liu X (2007). Drug delivery strategies for poorly water-soluble drugs. Expert Opinion on Drug Delivery, 4(4), 403–416. [PubMed: 17683253]

Fandaruff C, Araya-Sibaja AM, Pereira RN, Hoffmeister CRD, Rocha HVA, & Silva MAS (2014). Thermal behavior and decomposition kinetics of efavirenz under isothermal and non-isothermal conditions. Journal of Thermal Analysis and Calorimetry, 115(3), 2351–2356.

Filho R, Franco P, Conceição E, & Leles M (2009). Stability studies on nifedipine tablets using thermogravimetry and differential scanning calorimetry. Journal of Thermal Analysis and Calorimetry, 97(1), 343–347.

Friedrich H, Nada A, & Bodmeier R (2005). Solid state and dissolution rate characterization of co-ground mixtures of nifedipine and hydrophilic carriers. Drug Development and Industrial Pharmacy, 31(8), 719–728. [PubMed: 16221606]

Friesen DT, Shanker R, Crew M, Smithey DT, Curatolo WJ, & Nightingale JAS (2008). Hydroxypropyl methylcellulose acetate succinate-based spray-dried dispersions: an overview. Molecular Pharmaceutics, 5(6), 1003–1019. [PubMed: 19040386]

Gao P, & Shi Y (2012). Characterization of supersaturatable formulations for improved absorption of poorly soluble drugs. The AAPS Journal, 14(4), 703–713. [PubMed: 22798021]

Hancock BC, York P, & Rowe RC (1997). The use of solubility parameters in pharmaceutical dosage form design. International Journal of Pharmaceutics, 148(1), 1–21.

Haware RV, Vinjamuri BP, Gavireddi M, Dave VS, Gupta D, Chougule MB, & Stagner WC (2019). Physical properties and solubility studies of Nifedipine-PEG 1450/HPMCAS-HF solid dispersions. Pharmaceutical Development and Technology, 24(5), 550–559. [PubMed: 30175691]

Ilevbare GA, Liu H, Edgar KJ, & Taylor LS (2012a). Inhibition of solution crystal growth of ritonavir by cellulose polymers–factors influencing polymer effectiveness. CrystEngComm, 14(20), 6503–6514.

Ilevbare GA, Liu H, Edgar KJ, & Taylor LS (2012b). Understanding Polymer Properties Important for Crystal Growth Inhibition Impact of Chemically Diverse Polymers on Solution Crystal Growth of Ritonavir. Crystal Growth & Design, 12(6), 3133–3143.

Kalepu S, & Nekkanti V (2015). Insoluble drug delivery strategies: review of recent advances and business prospects. Acta Pharmaceutica Sinica B, 5(5), 442–453. [PubMed: 26579474]

Kallakunta VR, Patil H, Tiwari R, Ye X, Upadhye S, Vladyka RS, … Repka MA (2019). Exploratory studies in heat-assisted continuous twin-screw dry granulation: A novel alternative technique to conventional dry granulation. International Journal of Pharmaceutics, 555, 380–393. 10.1016/j.ijpharm.2018.11.045 [PubMed: 30458256]

Kallakunta VR, Sarabu S, Bandari S, Batra A, Bi V, Durig T, & Repka MA (2019). Stable amorphous solid dispersions of fenofibrate using hot melt extrusion technology: Effect of formulation and process parameters for a low glass transition temperature drug. Journal of Drug Delivery Science and Technology, 101395.

Kallakunta VR, Sarabu S, Bandari S, Tiwari R, Patil H, & Repka MA (2019). An update on the contribution of hot-melt extrusion technology to novel drug delivery in the twenty-first century: part I. Expert Opinion on Drug Delivery, 16(5), 539–550. [PubMed: 31007090]

Konno H, Handa T, Alonzo DE, & Taylor LS (2008). Effect of polymer type on the dissolution profile of amorphous solid dispersions containing felodipine. European Journal of Pharmaceutics and Biopharmaceutics, 70(2), 493–499. [PubMed: 18577451]

Kothari K, Ragoonanan V, & Suryanarayanan R (2014). The role of drug–polymer hydrogen bonding interactions on the molecular mobility and physical stability of nifedipine solid dispersions. Molecular Pharmaceutics, 12(1), 162–170. [PubMed: 25426538]

Leite RDS, Macedo RDO, Torres SM, Batista CCN, Baltazar LDO, Neto SAL, & De Souza FS (2013). Evaluation of thermal stability and parameters of dissolution of nifedipine crystals. Journal of Thermal Analysis and Calorimetry, 111(3), 2117–2123.

Lipinski C (2002). Poor aqueous solubility—an industry wide problem in drug discovery. Am Pharm Rev, 5(3), 82–85.

Ma X, Huang S, Lowinger MB, Liu X, Lu X, Su Y, & Williams RO III (2019). Influence of mechanical and thermal energy on nifedipine amorphous solid dispersions prepared by hot melt extrusion: Preparation and physical stability. International Journal of Pharmaceutics, 561, 324–334. [PubMed: 30858115]

Macêdo R, Gomes do Nascimento T, Soares Aragão C, & Barreto Gomes A (2000). Application of thermal analysis in the characterization of anti-hypertensive drugs. Journal of Thermal Analysis and Calorimetry, 59(3), 657–661.

Marasini N, Tran TH, Poudel BK, Cho HJ, Choi YK, Chi S-C, … Kim JO (2013). Fabrication and evaluation of pH-modulated solid dispersion for telmisartan by spray-drying technique. International Journal of Pharmaceutics, 441(1–2), 424–432. [PubMed: 23174408]

Mendonsa N, Almutairy B, Kallakunta VR, Sarabu S, Thipsay P, Bandari S, & Repka MA (2019). Manufacturing strategies to develop amorphous solid dispersions: An overview. Journal of Drug Delivery Science and Technology, 101459.

Pawar J, Tayade A, Gangurde A, Moravkar K, & Amin P (2016). Solubility and dissolution enhancement of efavirenz hot melt extruded amorphous solid dispersions using combination of polymeric blends: a QbD approach. European Journal of Pharmaceutical Sciences, 88, 37–49. [PubMed: 27049050]

Pinto EC, Cabral LM, & de Sousa VP (2014). Development of a discriminative intrinsic dissolution method for Efavirenz. Dissolut. Technol, 21, 31–40.

Pinto JMO, Leão AF, Riekes MK, França MT, & Stulzer HK (2018). HPMCAS as an effective precipitation inhibitor in amorphous solid dispersions of the poorly soluble drug candesartan cilexetil. Carbohydrate Polymers, 184, 199–206. [PubMed: 29352911]

Repka MA, Bandari S, Kallakunta VR, Vo AQ, McFall H, Pimparade MB, & Bhagurkar AM (2018). Melt extrusion with poorly soluble drugs–an integrated review. International Journal of Pharmaceutics, 535(1–2), 68–85. [PubMed: 29102700]

Sarabu S, Bandari S, Kallakunta VR, Tiwari R, Patil H, & Repka MA (2019). An update on the contribution of hot-melt extrusion technology to novel drug delivery in the twenty-first century: part II. Expert Opinion on Drug Delivery, 16(6), 567–582. [PubMed: 31046479]

Sarode AL, Obara S, Tanno FK, Sandhu H, Iyer R, & Shah N (2014). Stability assessment of hypromellose acetate succinate (HPMCAS) NF for application in hot melt extrusion (HME). Carbohydrate Polymers, 101, 146–153. [PubMed: 24299759]

Sarode AL, Sandhu H, Shah N, Malick W, & Zia H (2013). Hot melt extrusion (HME) for amorphous solid dispersions: predictive tools for processing and impact of drug–polymer interactions on supersaturation. European Journal of Pharmaceutical Sciences, 48(3), 371–384. [PubMed: 23267847]

Semjonov K, Kogermann K, Laidmäe I, Antikainen O, Strachan CJ, Ehlers H, … Heinämäki J (2017). The formation and physical stability of two-phase solid dispersion systems of indomethacin in supercooled molten mixtures with different matrix formers. European Journal of Pharmaceutical Sciences, 97, 237–246. [PubMed: 27890595]

Sun DD, & Lee PI (2013). Evolution of supersaturation of amorphous pharmaceuticals: the effect of rate of supersaturation generation. Molecular Pharmaceutics, 10(11), 4330–4346. [PubMed: 24066837]

Sun DD, & Lee PI (2015). Evolution of supersaturation of amorphous pharmaceuticals: nonlinear rate of supersaturation generation regulated by matrix diffusion. Molecular Pharmaceutics, 12(4), 1203–1215. [PubMed: 25775257]

Tanaka R, Hanabusa H, Kinai E, Hasegawa N, Negishi M, & Kato S (2008). Intracellular efavirenz levels in peripheral blood mononuclear cells from human immunodeficiency virus-infected individuals. Antimicrobial Agents and Chemotherapy, 52(2), 782–785. [PubMed: 18070970]

Tang XC, Pikal MJ, & Taylor LS (2002). A spectroscopic investigation of hydrogen bond patterns in crystalline and amorphous phases in dihydropyridine calcium channel blockers. Pharmaceutical Research, 19(4), 477–483. [PubMed: 12033383]

Tanno F, Nishiyama Y, Kokubo H, & Obara S (2004). Evaluation of hypromellose acetate succinate (HPMCAS) as a carrier in solid dispersions. Drug Development and Industrial Pharmacy, 30(1), 9–17. [PubMed: 15000425]

Tominaga K (2013). Effect of manufacturing methods used in the stability of amorphous solid solutions and predictions to test them.

Tsume Y, Mudie DM, Langguth P, Amidon GE, & Amidon GL (2014). The Biopharmaceutics Classification System: subclasses for in vivo predictive dissolution (IPD) methodology and IVIVC. European Journal of Pharmaceutical Sciences, 57, 152–163. [PubMed: 24486482]

Ueda K, Higashi K, Yamamoto K, & Moribe K (2013). Inhibitory effect of hydroxypropyl methylcellulose acetate succinate on drug recrystallization from a supersaturated solution assessed using nuclear magnetic resonance measurements. Molecular Pharmaceutics, 10(10), 3801–3811. [PubMed: 24025080]

Ueda K, Higashi K, Yamamoto K, & Moribe K (2014). The effect of HPMCAS functional groups on drug crystallization from the supersaturated state and dissolution improvement. International Journal of Pharmaceutics, 464(1–2), 205–213. [PubMed: 24440403]

Van Der Lee R, Pfaffendorf M, Koopmans RP, Van Lieshout JJ, Van Montfrans GA, & Van Zwieten PA (2001). Comparison of the time courses and potencies of the vasodilator effects of nifedipine and felodipine in the human forearm. Blood Pressure, 10(4), 217–222. [PubMed: 11800060]

Vasconcelos T, Sarmento B, & Costa P (2007). Solid dispersions as strategy to improve oral bioavailability of poor water soluble drugs. Drug Discovery Today, 12(23–24), 1068–1075. [PubMed: 18061887]

Williams HD, Trevaskis NL, Charman SA, Shanker RM, Charman WN, Pouton CW, & Porter CJ (2013). Strategies to address low drug solubility in discovery and development. Pharmacological Reviews, 65(1), 315–499. [PubMed: 23383426]

Zhang Q, Zhao Y, Zhao Y, Ding Z, Fan Z, Zhang H, … Han J (2018). Effect of HPMCAS on recrystallization inhibition of nimodipine solid dispersions prepared by hot-melt extrusion and dissolution enhancement of nimodipine tablets. Colloids and Surfaces B: Biointerfaces, 172, 118–126. [PubMed: 30144623]

Article Highlights:

- Amorphous solid dispersions were prepared using HPMCAS via hot melt extrusion
- NFD was solubilized better by HPMCAS grades compared to EFZ
- Drug physicochemical properties affected the dissolution efficiency of the polymer
- Substitutions on polymer grades had a significant effect on supersaturation maintenance
- Solid state hydrophobic interactions between the drug and acetyl groups of the polymers govern the dissolution and supersaturation maintenance
- HPMCAS MG grade exhibited greater supersaturation maintenance compared to LG and HG grades.

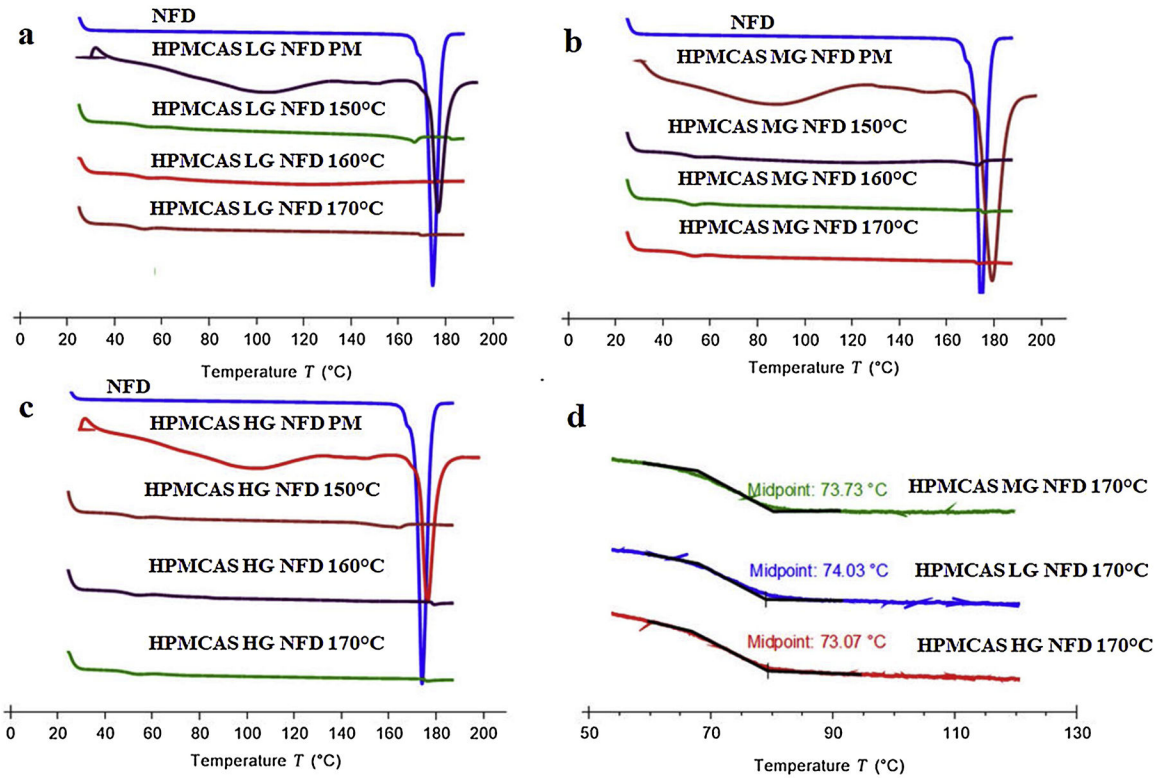

Figure 1.

DSC thermograms of NFD, HPMCAS NFD PM, HPMCAS NFD formulations (a, b and c) and miscibility test (d) data of HPMCAS NFD samples

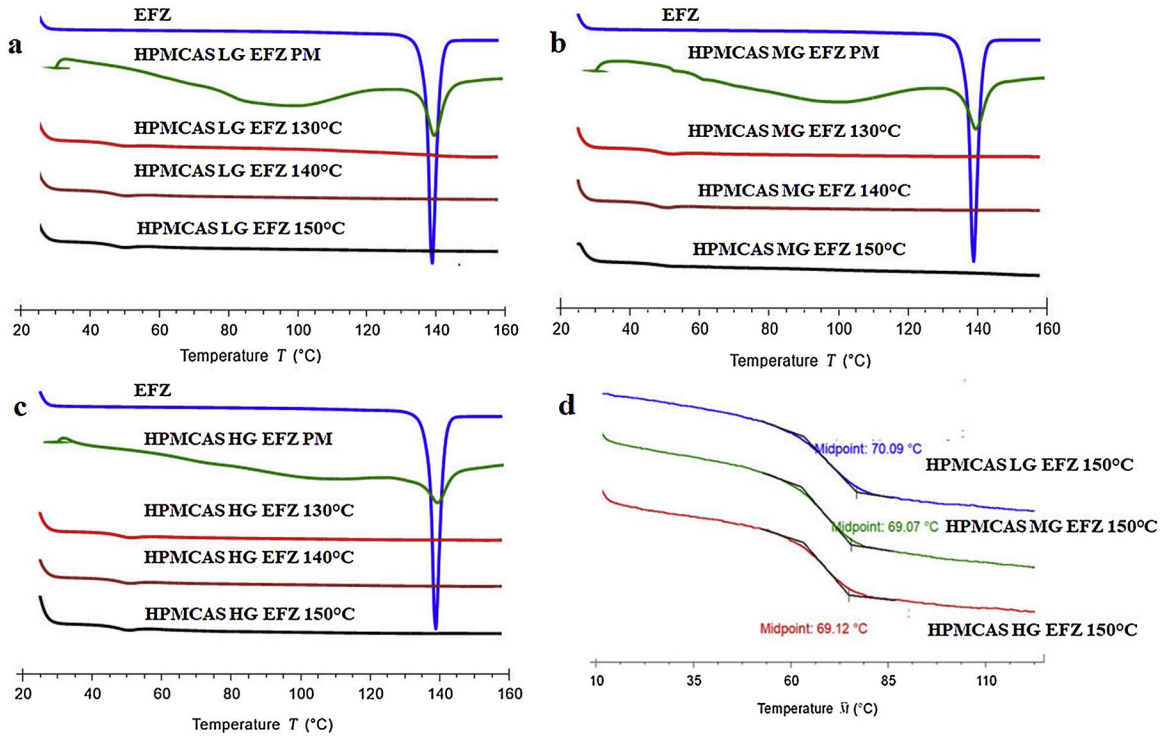

Figure 2.

DSC thermograms of EFZ, HPMCAS EFZ PM and HPMCAS EFZ formulations (a, b and c) and miscibility test (d) data of HPMCAS-EFZ samples

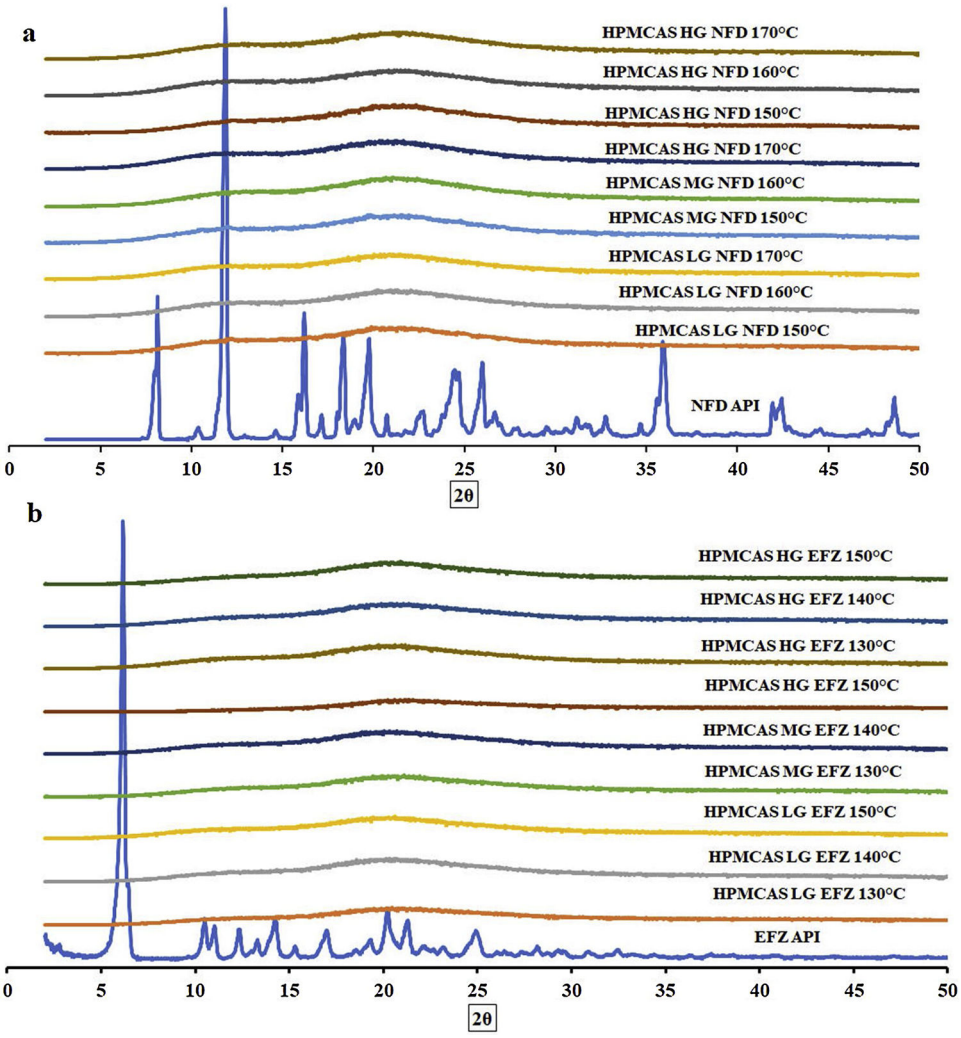

Figure 3.

PXRD graphs for a) Pure NFD and HPMCAS-NFD formulations extruded at temperatures 150-170°C and b) Pure EFZ and HPMCAS-EFZ formulations extruded at temperatures 130-150°C

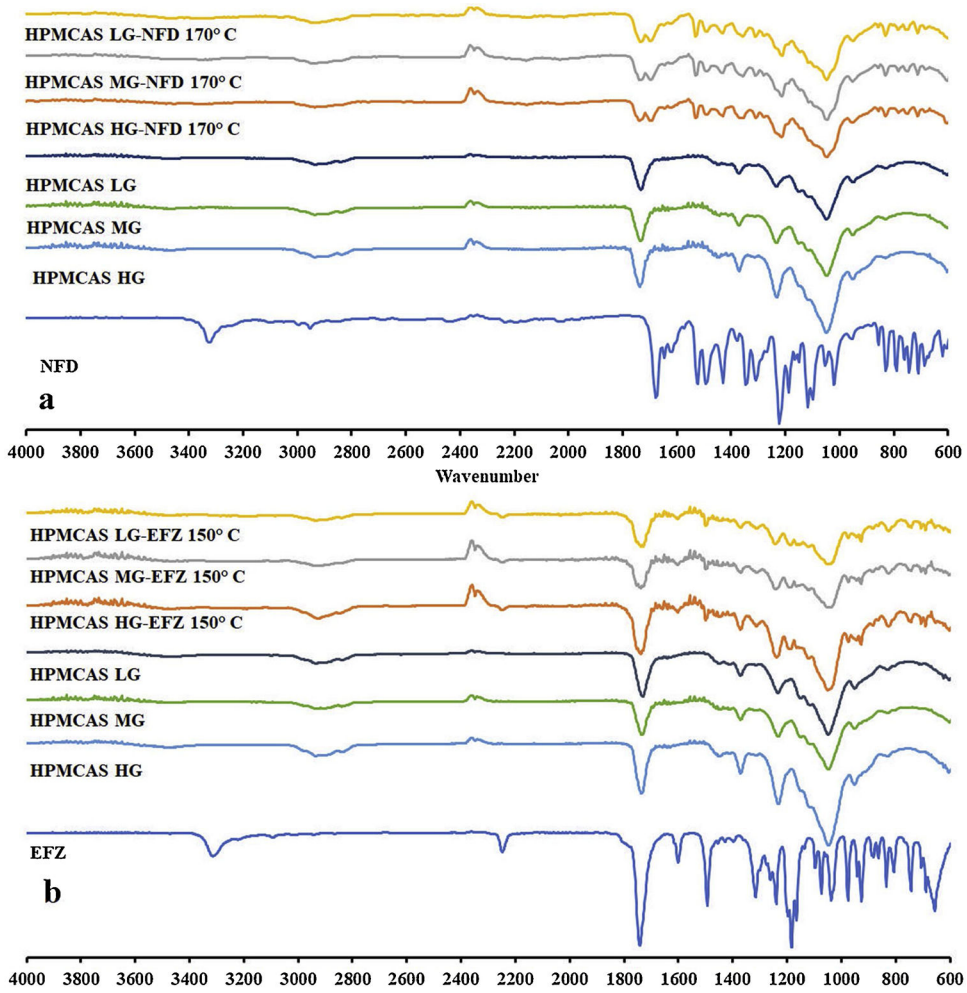

Figure 4.

FTIR spectra of pure NFD, EFZ, pure polymers and respective formulations; a) NFD with three polymer grades of HPMCAS b) EFZ with three polymer grades of HPMCAS

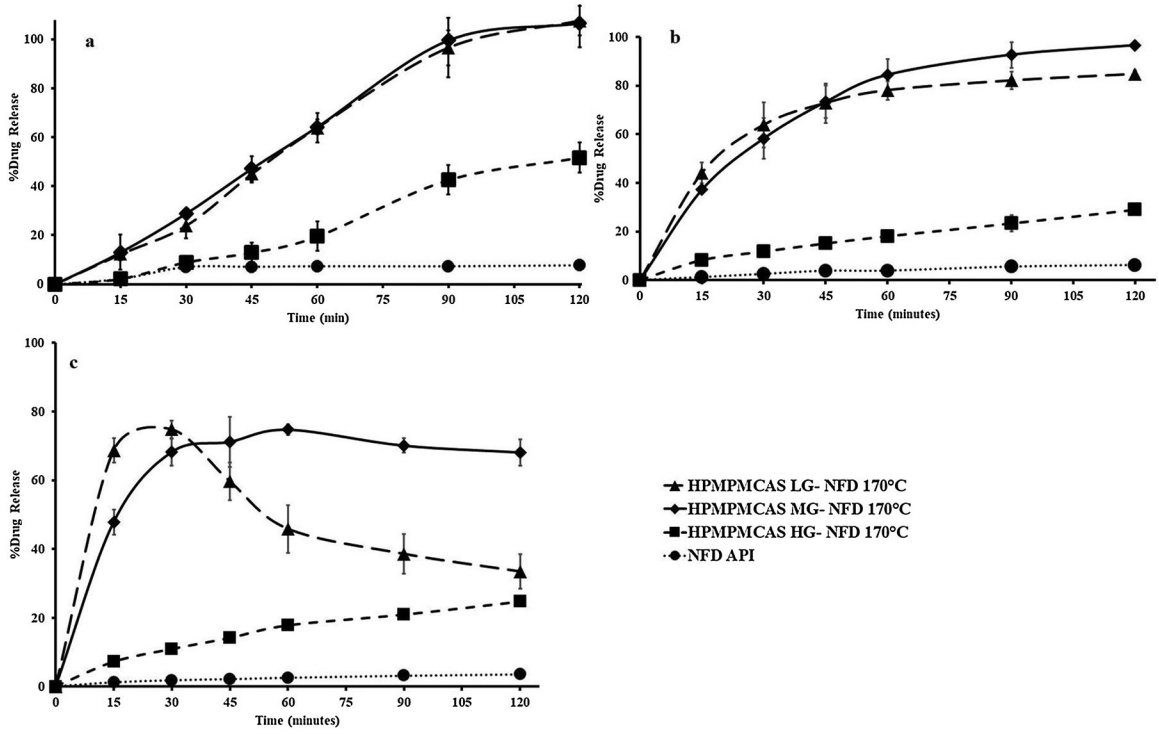

Figure 5.

Dissolution profiles of HPMCAS LG-NFD, MG-NFD, HG-NFD formulations and NFD API; a) Dissolution at 20 mg equivalent dose, b) Dissolution at 67.5 mg equivalent dose, and c) Dissolution at 135 mg equivalent dose of NFD

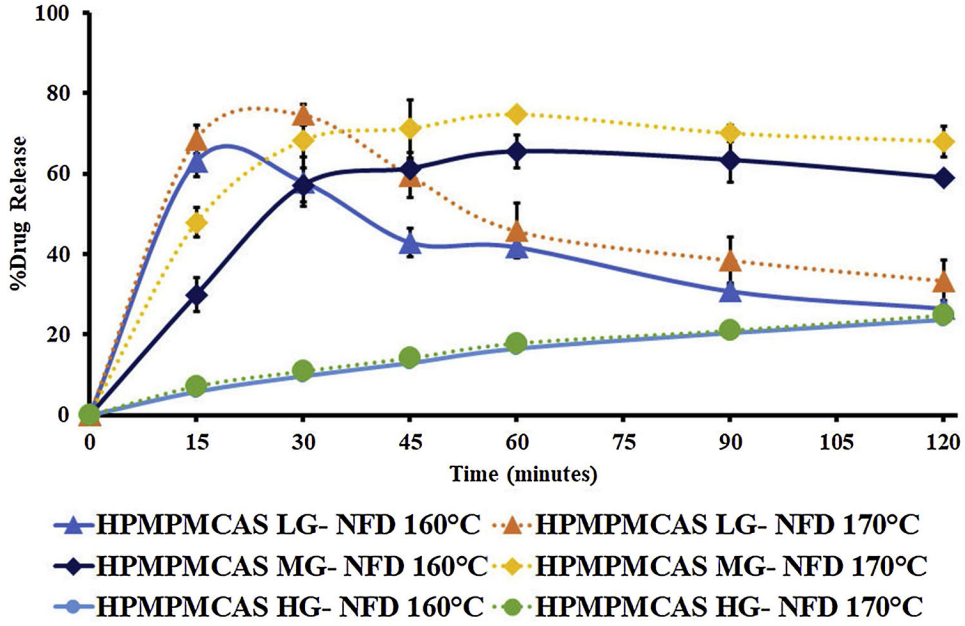

Figure 6.
Effect of processing temperature on dissolution profiles of HPMCAS-NFD formulations

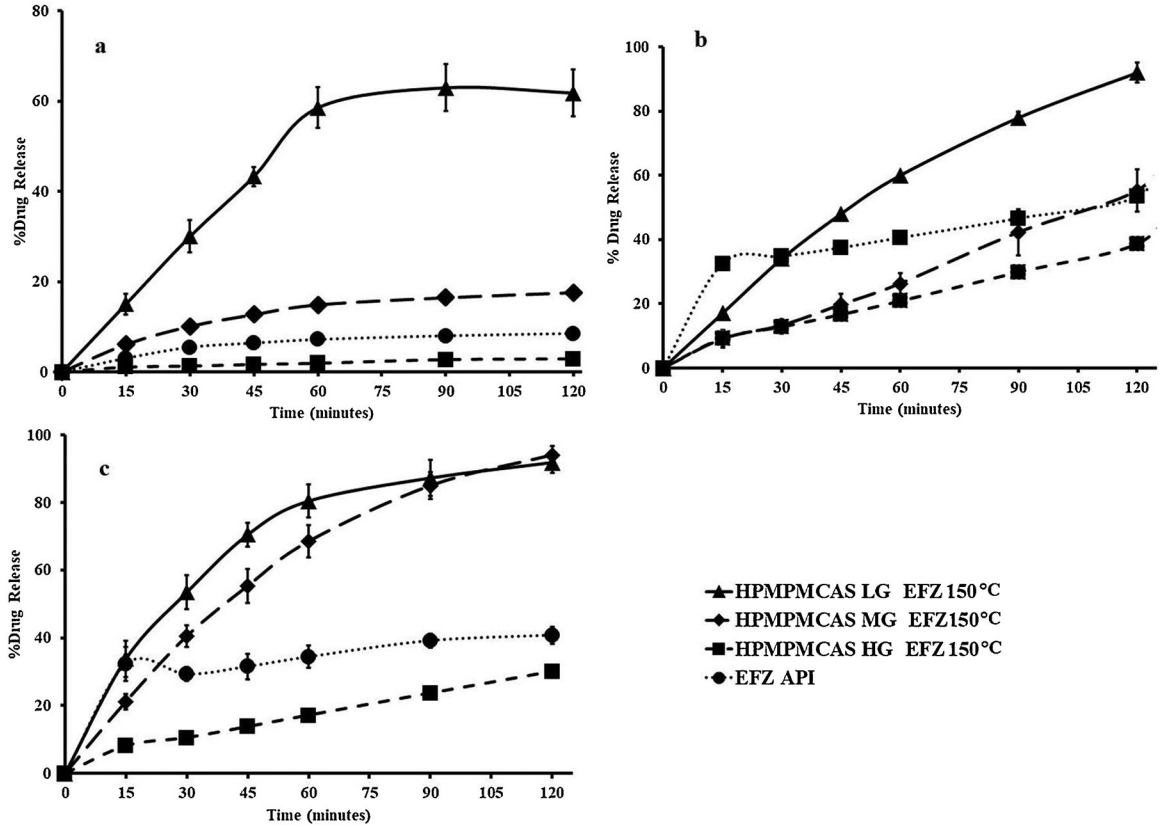

Figure 7.

Dissolution profiles of HPMCAS (LG, MG and HG)-EFZ formulations and pure EFZ in a) pH 6.8 phosphate buffer, b) pH 6.8 phosphate buffer + 1% SLS and c) pH 6.8 phosphate buffer + 0.25% SLS

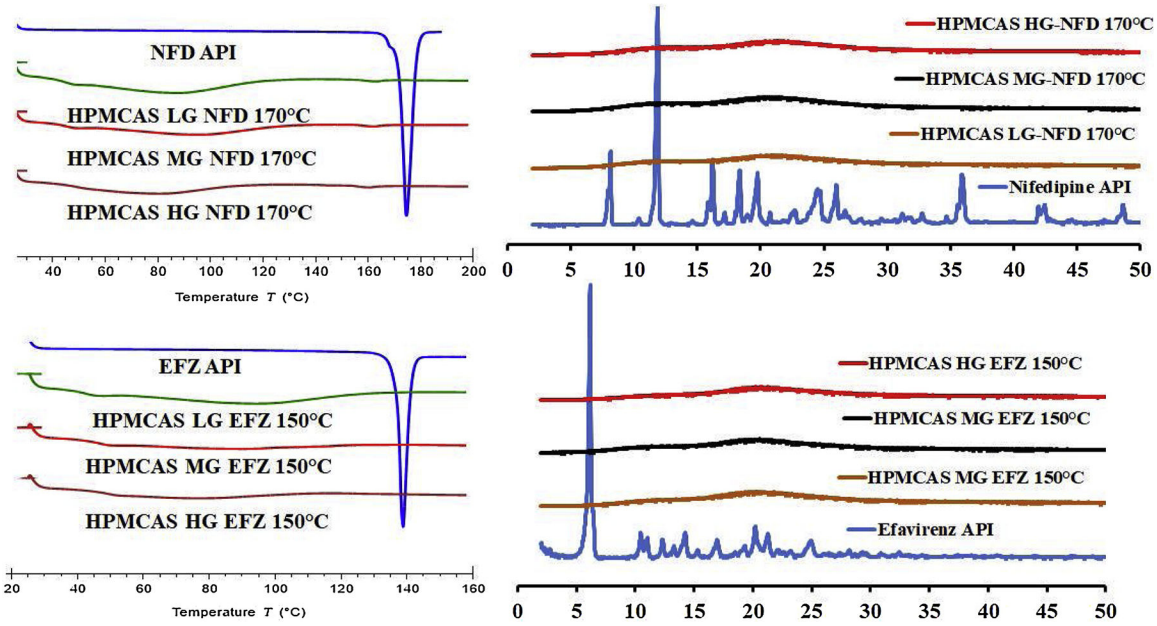

Figure 8.

DSC thermograms and PXRD graphs of HPMCAS-NFD and HPMCAS-EFZ formulations after 3 months of storage at accelerated stability conditions and pure API

Table. 1

a) Degree of substitution and physicochemical properties of HPMCAS grades, b) Extrusion process temperature and torque values for pure polymer and formulations

HPMCAS Grade	Acetyl- (%)	Succinoyl- (%)	Methoxyl- (%)	Hydroxy propoxy- (%)	Tg (°C)	pH solubility	MW	Melt Viscosity (mPa.S)
LG	5-9	14-18	20-24	5-9	119	5.5-6	114,700	2.4-3.6
MG	7-11	10-14	21-25	5-9	120	6-6.5	103,200	2.4-3.6
HG	10-14	4-8	22-26	6-10	122	>6.8	75,100	2.4-3.6

Name	**Torque values (in Nm) at different extrusion temperatures (° C)**						
	130	**140**	**150**	**160**	**170**	**180**	**190**
HPMCAS LG	Exceeded instrument maximum (>12 Nm)				> 10.2	7.8-8.5	6.6-7.2
HPMCAS MG	>12	>12	>12	> 10	8.0-8.4	6.7-7.2	NA
HPMCAS HG	>12	>12	>12	> 10	7.2-7.6	6-6.4	NA
HPMCAS LG-NFD	>12	10.2-10.5	7.0-7.2	5.5-6.1	5.0-5.6	4.8-5.3	NA
HPMCAS MG-NFD	>12	10.0-10.2	6.6-6.8	5.0-6.0	4.9-5.4	4.6-5.0	NA
HPMCAS HG-NFD	>12	9.5-9.8	5.8-6.1	4.8-5.4	4.3-4.6	3.6-4.0	NA
HPMCAS LG-EFZ	5.4-6.0	4.3-4.4	3.2-3.6	NA	NA	NA	NA
HPMCAS MG-EFZ	5.2-5.4	3.7-3.8	3.2-3.4	NA	NA	NA	NA
HPMCAS HG-EFZ	4.6-4.8	3.4-3.7	3.0-3.2	NA	NA	NA	NA

Table 2.

Summary of dissolution parameters for NFD API and NFD formulations (n=6); DE15, DE30 and DE60 are dissolution efficiency values at 15,30 and 60 minutes; MDR and IDR are mean dissolution time, mean dissolution rate and initial dissolution rate respectively;

Sample	DE_{15}	DE_{30}	DE_{60}	MDR	IDR
LG-NFD @ 20 mg dose	6.51	13.72	30.28	0.63	0.87
MG-NFD @ 20 mg dose	6.12	12.08	28.24	0.60	0.82
HG-NFD @ 20 mg dose	1.10	3.33	8.45	0.22	0.15
NFD API @ 20 mg dose	1.09	2.83	4.95	0.09	0.15
LG-NFD @ 67.5 mg dose	22.06	38.03	55.08	1.20	2.94
MG-NFD@ 67.5mg dose	18.86	33.42	52.98	1.12	2.51
HG-NFD@ 67.5 mg dose	2.11	3.59	5.55	0.25	0.55
NFD API @ 67.5 mg dose	0.62	1.26	1.91	0.05	0.08
LG-NFD @ 135 mg dose	34.31	53.01	56.49	1.44	4.58
MG-NFD @ 135 mg dose	23.91	40.97	56.14	1.22	3.19
HG-NFD @ 135 mg dose	3.61	6.34	10.32	0.23	0.48
NFD API @ 135 mg dose	0.62	1.08	1.4	0.05	0.08